

Typical uncertainty analysis of acoustic discharge measurements by multipath flow meters in hydropower applications

P. Gruber¹

¹*pgconsult.ch gmbh, Grenzacherweg 116, 4125 Riehen, Switzerland*
E-mail: pgconsult@gmx.ch, www.pgconsult.ch

Abstract

The acoustic discharge measurement (ADM) with multipath arrangements is a proven method for measuring the flow in hydropower plants. The accuracy of such a measurement system is dependent on various quantities related to the installation, the flow conditions (pump and turbine mode) and the determination of the path velocities by transit time t_{abs} and transit time difference between upstream and downstream time measurements. This main focus of this analysis on min/max and statistical error propagation of the geometrical inaccuracies of all relevant geometrical quantities as positions, lengths, heights (as measured on site after the installation) and from the determination of time measurements. Two types of probability density functions (pdf) approaches are used for representing the uncertainty in a statistical way: a Gaussian and a uniform pdf. The error propagation is split in two parts in sequence. The first part determines the error propagation for the path velocity, the second part the uncertainty in the flow (rate) Q . The error analysis assumes that the cross flow is zero or ideally compensated, such that the axial layer velocities can be used. Furthermore the dependency of the uncertainty on the flow velocity is shown.

The resulting uncertainty is then combined with all the other uncertainties as mentioned above to obtain an estimate of the 95% confidence interval of the flow measurement. The Nant de Drance installation is presented as an example. A discussion at the end shows that different analysis methods can be chosen and combined depending on the chosen assumptions on the error types (min/max, Gaussian, independence) of the error sources.

1. Introduction

1.1 Multi-path configuration

The standard IEC 60041:1991 [1] describes the two crossed vertical planes with crossed paths at four horizontal layers for hydropower applications as is shown in Figure 1. On each path transit times t_d , t_u ([1] resp $t_{forward}$, $t_{reversed}$ [9]) y_d (resp $y_{forward}$) and y_u (resp $y_{reversed}$) sent in forward and reverse direction of the flow are recorded. The time difference between the two transit times allows to determine the mean projected flow velocity on the path. In a crossed path configuration possible cross flow components can ideally be completely compensated.

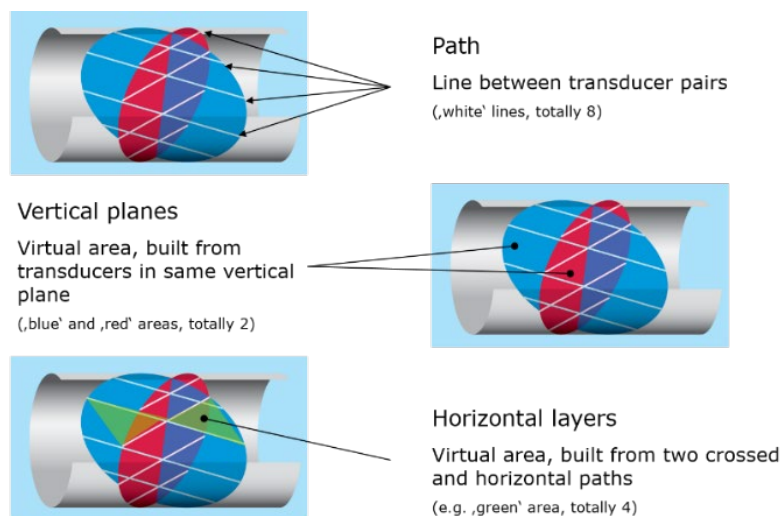


Figure 1: crossed 8-path configuration in 2 vertical planes (source: training Rittmeyer AG, Baar, Switzerland)

An acoustic discharge flow meter has therefore to process acoustic signals acquired at a high sampling frequency (f_s or $T_s = \frac{1}{f_s}$) of 10 to 100 MHz and to produce an output flow measurement Q at a much lower rate of typically $f_{output} = 1\text{Hz}$ resp. $T_{output} = \frac{1}{f_{output}} = 1\text{sec}$. In order to achieve that, the needed signal processing can be split in at least two big blocks as shown in Figure 2: a fast processing block I at the front end with extensive digital filtering and signal processing for each path, producing axial path velocities at an intermedium rate T_1 , and a second block II adding by a weighted sum all the axial path velocities, producing measurement values of Q at an output rate T_{output} .

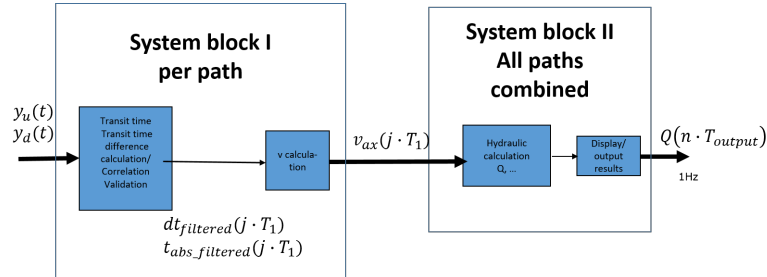


Figure 2: signal processing chain

1.2 Uncertainty issues

The determination as described above is an accurate method for obtaining the flow in ideal conditions. Ideal means that the positioning of the 16 transducers (2 per path) are exactly at the positions as required by the numerical integration method chosen (see Table in [3]), which means that all geometrical quantities are accurate and the velocity determination is not affected by uncertainties in timing, flow and ambient conditions. For the installation of an ADM system the geometry of the pipe and the positions of the transducers have to be measured after the installation. Inaccuracy of the installation procedure leads to numerous potentially deterministic geometric systematic errors in an 8-path configuration. The question arises how to handle these. A reasonable procedure is to simplify the problem as much as can be tolerated. The method chosen for error propagation also depends heavily on what assumptions can be made regarding the above errors. Therefore, smaller or larger uncertainty bands for the flow measurement of Q can be derived. A detailed analysis of which assumptions are most appropriate cannot be found in general terms, but must be individually and carefully selected for each site.

1.3 outline of the paper

The paper starts with the signal processing needed for determining the velocity for a single path. The challenge here is to get a good estimate for the transit time difference dt . As a signal processing example, the often used correlation method for deriving dt is presented. Then the complete formulas are given for an 8-path installation for the axial layer velocities and the total flow Q . A list of error sources is presented for the overall installation. For the error propagation some simplifications are carried out in order to reduce the complexity. The error propagation is done for a min/max error and statistical error presentation with two different choices of the probability density function of the error sources. Two chosen methods are then applied to an existing installation at Nant de Drance in Switzerland. The overall uncertainty including all the other error sources is done in a min/max and statistical way. The paper ends with a conclusion including a discussion on how to deal with the various sources of error.

2 Determination of the axial path velocities

2.1 Single path/crossed paths

Figure 3 shows the situation for a single and crossed path application for one layer. For each path the axial path velocity can be determined by

$$v_{ax_{path_i}} = \frac{L_i \cdot dt_i}{2 \cdot \cos(\varphi_i) \cdot t_{u_i} \cdot t_{d_i}} \quad i=1, \dots, 8 \quad (1)$$

The velocities are average path velocities along the paths. For a crossed arrangement, as shown in Figure 1, there are only 4 axial layer velocities $v_{ax,i}$, $i=1, \dots, 4$, where these are a weighted combination of the two axial path velocity of the corresponding layer

$$v_{ax,i} = \frac{v_{ax_{path_i}} \cdot \tan(\varphi_{i+4}) + v_{ax_{path_{i+4}}} \cdot \tan(\varphi_i)}{\tan(\varphi_i) + \tan(\varphi_{i+4})} \quad i=1, \dots, 4 \quad (2)$$

with φ_i assigned to plane A and φ_{i+4} to plane B.

If $\varphi_{i+4} = \varphi_i$ equation (2) is written as the average of the two axial path velocities of the layer.

$$v_{ax,i} = \frac{v_{axpath,i} + v_{axpath,i+4}}{2} \quad i=1, \dots, 4 \quad (3)$$

To calculate the transverse velocity $v_{tr,i}$ of each layer, the angle α is needed as well as the axial path velocities and angles of each plane as shown in Figure 3:

$$\tan \alpha = \frac{\cos(\varphi_i) \cdot v_{axpath,i} - \cos(\varphi_{i+4}) \cdot v_{axpath,i+4}}{\tan(\varphi_{i+4}) \cdot \cos(\varphi_i) \cdot v_{axpath,i} + \tan(\varphi_i) \cdot \cos(\varphi_{i+4}) \cdot v_{axpath,i+4}} \quad (3a) \quad v_{tr,i} = v_{ax,i} \cdot \tan \alpha \quad (3b)$$

If $\varphi_{i+4} = \varphi_i$ equation (3a) is written as $\tan \alpha = \frac{(v_{axpath,i} - v_{axpath,i+4})}{\tan(\varphi_i) \cdot (v_{axpath,i} + v_{axpath,i+4})}$

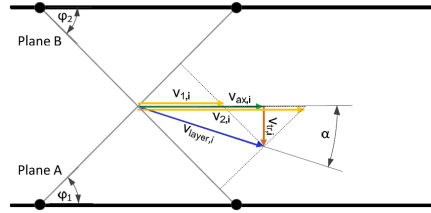


Figure 3: single and crossed path configuration ($v_{1,j} = v_{axpath,i}$, $v_{2,j} = v_{axpath,i+4}$)

Figure 4 shows the main signal processing steps in block I for obtaining the axial path velocity: The analog front end consists of an anti-aliasing band pass filter with center sensor frequency and variable gain. The gain is controlled by the automatic gain control block AGC that adjusts the gain of the filter such that the amplitude of the signal lies in a safe range of the A/D converter. The signal analysis block guarantees that the signal is not saturated and not too small. The A/D converter has a sampling frequency that is at least 10 times higher as the sensor frequency and a quantization of 14 to 16 bit. Pulses are sent in a periodic interval (ping rate) several times per second depending on the path length. The receive signal detection block finds the travelling signal pulse by listening to the received signal in a specified time range. The next block analyses the signal quality by retrieving characteristic values and cut out a signal window for further processing in the correlation block. The transit times are found by analyzing the signal envelope and from that the start time of the signal window. Variation of the obtained values is inevitable. Therefore, nonlinear low-pass filtering and validity checking is required over a range of determined values. An error bound of around

$$\Delta t_d = \Delta t_u = 0.5 \mu s \quad (4)$$

for the usual sensor frequencies can thus be achieved. The physics of the pulse propagation in flowing water indicates that the accuracy needed for the estimation of the transit times is allowed to be a factor of 10^3 or more, worse than the accuracy needed for the determination of the transit time difference in order to get good results ([2]). Several validity checks are done before the final calculation of the velocity.

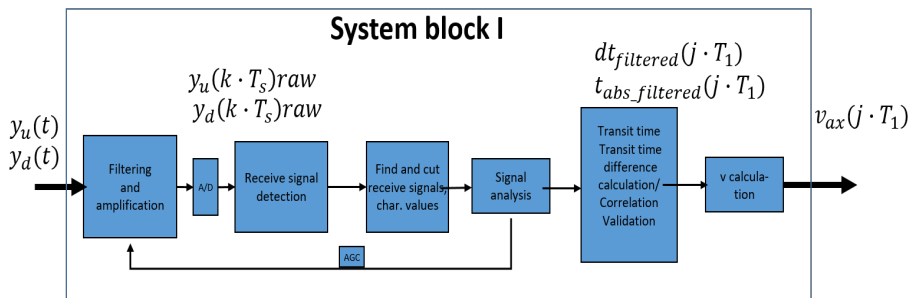


Figure 4: signal processing in block I

2.2 Determination of transit time difference dt

The important dt determination is shown here by the correlation between forward and return signal. The two discrete signals $y_d(k)$ and $y_u(k)$ are first made offset free by subtraction of the mean of each signal in the corresponding signal window. The window size N of the two signals is chosen to be the same. Then one gets for the correlation of the offset free signals $\bar{y}_d(k)$ and $\bar{y}_u(k)$

$$Corr(\bar{y}_d(k), \bar{y}_u(k))_j = \frac{1}{N} \sum_{k=0}^{N-1} \bar{y}_d(k) \cdot \bar{y}_u(j+k) \quad j=0, \dots, 2N-1 \quad (5)$$

The shift of the occurrence of the correlation maximum to the center of the correlation is the time shift between the two signals. The principle is shown in Figure 5 with two sinusoidal signals with amplitude 1 and of period 100 (total length 300) starting at $k=100$ and $k=500$. The total recorded length N is 1200. Obviously, the difference in the two signals is $dk=500-100=400$. The correlated signal has a length of 2400. The correlation function has the same frequency as the two original signals, a length of 600 and a symmetrical linearly rising and falling envelope with a distinct maximum of the correlation function. The maximum occurs at $k=800$, the time shift between the middle of the correlation window is $dk=1200-800=400$.

In the case of two acoustic pulses the situation is more complex. The positions of the two signal windows must be taken into account and the maximum of the continuous waveform lies in between the samples of the discrete correlation function. Therefore, more signal processing algorithms for filtering and interpolation are a must. Figure 6 shows two signals (adjusted in time shift for comparison with the maximum) of actual recorded acoustic pulses and their correlation. Although the shape of the pulses is different from the sinusoidal case, the correlation is very similar to the sinusoidal case. The individual pulses are nearly identical in shape. Therefore, the correlation function is strongly symmetrical. The jitter of the timing clock can be neglected. Variation of the obtained values, although much smaller than in the case of the transit time determination, is again inevitable. Thus, with adequate signal processing (again nonlinear low pass filtering validity checking) the error Δdt for the determination of dt can be assumed to be in the range of

$$\Delta dt = 1 \text{ to } 2 \text{ ns} \quad (6)$$

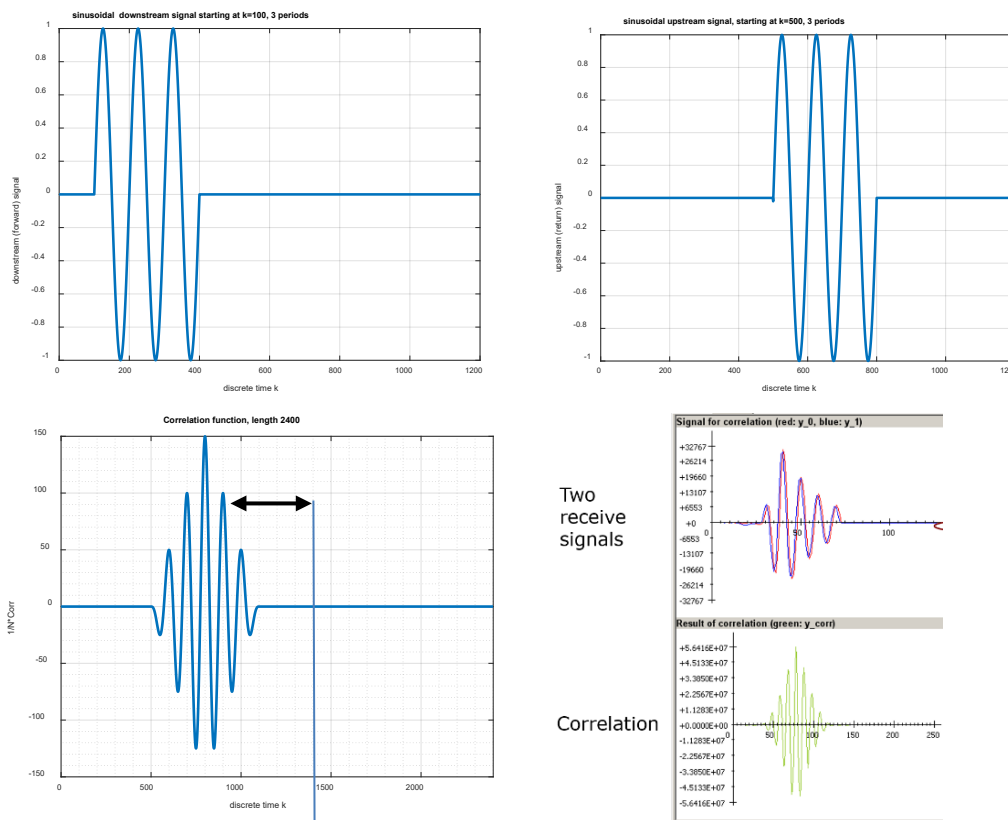


Figure 5&6: upper left and right: ideal down and upstream signal, lower right: correlation of the two signals, lower left: recorded up- and downstream signals and their correlation (source: Rittmeyer AG, Baar, Switzerland)

3 General formula of flow determination for 8-path configuration

After the determination of all the axial layer velocities, system block II calculates the flow Q at an output rate of e.g. 1 second. For this purpose, a summation formula is chosen that depends on the geometry of the measurement location. The equation for an 8-path application is

$$Q = \frac{D}{2} \sum_{i=1}^4 w_i b_i v_{ax,i} \quad (7)$$

$$\text{with the width } b_i = \frac{(L_i - L_{T_i}) \cdot \sin(\varphi_i) + (L_{i+4} - L_{T_{i+4}}) \cdot \sin(\varphi_{i+4})}{2} \quad i=1, \dots, 4 \quad (8)$$

where $L_{w,i} = (L_i - L_{T_i})$ is the path length wall to wall (L_{T_i} = average of protrusion length of the two transducers of path i , is usually < 0) (9)

The weights w_i $i=1, \dots, 4$ are given by the integration method (Gauss-Jacobi, Gauss-Legendre, OWICS, OWIRS, OWISS, see Table in [3],[4]).

Plugging equations (8) and (9) in equation (7) leads to a rather complicated expression for Q

$$Q = \frac{D}{2} \sum_{i=1}^4 w_i \left(\frac{(L_i - L_{T_i}) \cdot \sin(\varphi_i) + (L_{i+4} - L_{T_{i+4}}) \cdot \sin(\varphi_{i+4})}{2} \right) \left(\frac{\frac{L_i \cdot dt_i}{2 \cdot \cos(\varphi_i) \cdot t_{f_i} \cdot t_{r_i}} \tan(\varphi_{i+4}) + \frac{L_{i+4} \cdot dt_{i+4}}{2 \cdot \cos(\varphi_{i+4}) \cdot t_{d_{i+4}} \cdot t_{u_{i+4}}} \tan(\varphi_i)}{\tan(\varphi_i) + \tan(\varphi_{i+4})} \right) \quad (10)$$

4 Error sources

In section 2, errors have been discussed occurring in the determination of times needed for the determination of the velocity. However, this is only one of the sources of signal processing error required to determine the flow (see second entry in subsection (a) below). A flow measurement installation based on the acoustic discharge measurement method is exposed from an overall perspective to the following error sources (see also Standard IEC 60041:1991, annex J.7 [1]):

- a) Errors in the determination of the flow Q from the transit times: e_Q
 - Measurement of path lengths, path angles, path heights and pipe diameter
 - Determination of the absolute transit time and transit time differences
 - Determination of path velocities and total discharge Q
- b) Integration error: e_{int}
 - Transverse or cross flow components
 - Flow profile distortion
 - Special variations of flow field along the conduit in the measurement section
 - Type of integration method
- c) Protrusion error: e_{prot}
 - Flow distortion around the transducers due to the protrusion of the sensors
- d) Ambient influences: e_{amb}
 - Temperature
 - Speed of sound
 - Pressure
 - Air bubbles
 - Suspended sediment
- e) Unsteady flow conditions: $e_{unsteady}$
 - Periodic components
 - Non-stationary flow field
 - Random noise effects

There are three kinds of error contributions for several of the above errors:

- Spurious
- Systematic
- Random

The definition of these three types of errors can be found in the Standard IEC 60041:1991 section 6.2.3 [1].

The following uncertainty analysis discusses the following approaches:

- Error analysis with min/max error bands
- Statistical analysis with error propagation of standard deviations
- Combination of min/max and statistical approach

5 Uncertainty representation

Errors of directly measured quantities are represented with symmetrical error bands: $\pm\Delta$

In case of the min/max analysis, the full interval propagation is pursued. In case of a statistical approach, the systematic errors are treated in a statistical way.

If the systematic error of a measurement device is unknown, but bounded, an assumed symmetrical interval $\pm\Delta$ occurs. There are two reasonable ways to represent the systematic error in a statistical way when no further information about the error distribution is available:

- The interval $\pm\Delta$ may be assumed as a systematic uncertainty with a confidence level better than 95% for an assumed Gaussian distribution of a random variable x . This leads to the following relation between Δ and σ

$$E[x] = 0 \qquad \Delta \sim 2\sigma \qquad \sigma \sim \Delta/2 \quad (11)$$

- The systematic error is assumed to be uniformly distributed represented by the random variables (x) in the uncertainty band with the following mean and standard deviation (see [7] GUM, chapter 4)

$$E[x] = 0 \quad \sigma = \frac{\Delta}{\sqrt{3}} \quad (12)$$

This standard deviation is then used for a Gaussian distribution.

Here the second approach is pursued for measured geometrical and timing quantities, as it gives a more conservative estimation of the confidence level. Purely random uncertainties, as for instance the ambient influence, are represented by a Gaussian distribution of mean zero and specified σ .

Gaussian distributions are assumed for the statistical error propagation law for the derived quantities, so the above σ -values for Gaussian distributions are used. The uncertainty of a quantity y derived by the propagation law is then given by:

$$\text{Confidence interval for a probability of 95\%: } \pm 2\sigma_y \quad (13)$$

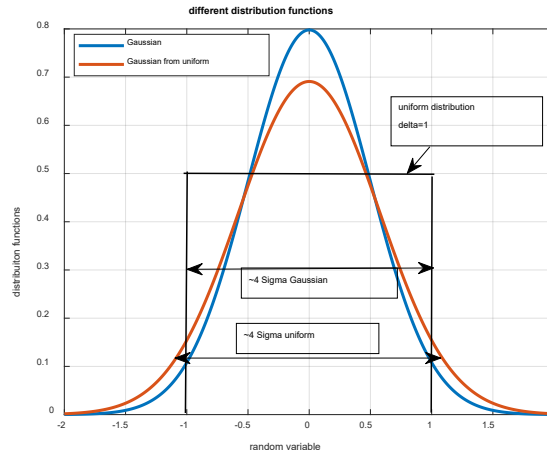


Figure 7: different probability density functions $\Delta=1$

Figure 7 shows the implication if the uniform probability distribution is used: the Gaussian equivalent shows a lower peak (~15%) and, as expected, from equation (11) and (12) a broader shape.

6 Error propagation min/max and statistical

6.1 Error sources for flow determination equation

A closer inspection of the equation (10) for the determination of Q reveals that Q is dependent on the following 49 parameters:

- 8 path lengths L_i
- 8 angles φ_i
- 8 absolute downstream (forward) t_{d_i}
- 8 upstream (return) transit times t_{u_i}
- 8 transit time differences dt_i
- 8 protrusions lengths L_{T_i}
- 1 diameter D .

That means one would have to perform 49 first derivatives for the linear error propagation law. It certainly will make sense to simplify the situation such that the problem can be reduced in number of variables and in consecutive separate equations.

6.2 Error propagation models

The approach follows roughly the argumentation of [5] (J. Hoffmann: Taschenbuch der Messtechnik). As is usually the case, the error propagation for small variations $\delta x_1, \delta x_2$ is done with a first order Taylor series expansion around a nominal point, e.g. $x_1 = \bar{x}_1, x_2 = \bar{x}_2$ for a function of two variables. Then one gets

$$y = f(x_1, x_2) \quad \delta y \cong \left. \frac{\partial f}{\partial x_1} \right|_{x_1, x_2} \cdot \delta x_1 + \left. \frac{\partial f}{\partial x_2} \right|_{x_1, x_2} \cdot \delta x_2 \quad (14)$$

As the sign of $\delta x_1, \delta x_2$ are not known for the further analysis all terms have to be taken positive in order to cover the conservative case in the min/max approach. This results in

$$\text{Min/max approach:} \quad \delta y \cong \left| \frac{\partial f}{\partial x_1} \right|_{x_1, x_2} \cdot |\delta x_1| + \left| \frac{\partial f}{\partial x_2} \right|_{x_1, x_2} \cdot |\delta x_2| = a_1 \cdot |\delta x_1| + a_2 \cdot |\delta x_2| \quad (15)$$

For the min/max approach δ will be replaced by Δ .

For a statistical approach (15) is squared and one gets with the definition of the variances of the assumed random variables $\delta y, \delta x_1, \delta x_2$ all with zero mean as

$$\begin{aligned} \sigma_y^2 &= E\{(\delta y)^2\}, \sigma_{x_1}^2 = E\{(\delta x_1)^2\}, \sigma_{x_2}^2 = E\{(\delta x_2)^2\} \\ \sigma_y^2 &= (\delta y)^2 = (a_1 \cdot \delta x_1 + a_2 \cdot \delta x_2)^2 = a_1^2 \cdot \sigma_{x_1}^2 + a_2^2 \cdot \sigma_{x_2}^2 + 2a_1 a_2 E\{\delta x_1 \cdot \delta x_2\} \\ \sigma_y^2 &= a_1^2 \cdot \sigma_{x_1}^2 + a_2^2 \cdot \sigma_{x_2}^2 + 2a_1 a_2 \sigma_{x_1} \sigma_{x_2} \cdot \rho \end{aligned} \quad (16)$$

where ρ the Pearson correlation coefficient lies between -1 and +1. In general, the product term cannot be neglected by adding only the first 2 products of equation (16), see also GUM [8]). To obtain maximal variance of y the assumption $\rho = 1$ must be made

$$\delta x_1 = \delta x_2 = \delta x \quad \text{resulting in} \quad \sigma_y^2 = (a_1 + a_2)^2 \cdot \sigma_x^2 \quad (17)$$

$$\text{For uncorrelated } \delta x_1 \text{ and } \delta x_2 \quad \sigma_y^2 = a_1^2 \cdot \sigma_{x_1}^2 + a_2^2 \cdot \sigma_{x_2}^2 \quad (18)$$

6.3 simplifications/assumptions

In the following a number of simplifications resulting from assumptions are performed in order to reduce the complexity of equation (10).

a) Introduction of t_{abs}

t_{abs_i} is introduced instead of $t_{d_i} t_{u_i}$ as the error contribution of inaccuracy in the transit times contributes are so little to the dt timing uncertainty. So, equation (1) can be written as

$$v_{ax_{path_i}} = \frac{L_i \cdot dt_i}{2 \cdot \cos(\varphi_i) \cdot t_{abs_i}^2} \quad i=1, \dots, 4 \quad (19)$$

For paths with approximately the same length the same nominal t_{abs} will be used (long and short paths separately).

b) Horizontal orientation of the layers

From the coordinates of the transducers/sensor positions a check of the orientation of the layers (assumed ideally horizontal) can be done. If the difference in the height coordinates is of the order of \sim mm, for most applications with pipe diameter of 2 meters or more, the error caused by assuming ideal conditions is negligible.

c) Assumption: No cross flow, resp. crossflow is ideally compensated

The cross flow component is usually one order or two smaller in magnitude compared to the axial flow component. Additionally, the cross path arrangement compensates the greatest part of the cross flow component. So, the assumption to neglect the cross flow influence for the error analysis is justified in most cases.

d) Ideal path lengths, weights and path angles, no protrusion,

The lengths and weights are chosen according to the ideal Gauss-Jacobi (G-J), resp. (G-L) positions. For a 4 layer configuration the width b_i at the Gauss-Jacobi heights and the inner and outer path lengths from wall to wall are given by (for most cases, ideal path angles for all paths can be assumed to be $\varphi = 45^\circ$) :

$$b_{in,G-J} = D \cos\left(\frac{\pi 18}{180}\right) \quad b_{out,G-J} = D \cos\left(\frac{\pi 54}{180}\right) \quad (20a,b)$$

$$L_{in,G-J} = b_{in,G-J} / \cos\left(\frac{\pi(90-\varphi)}{180}\right) \quad L_{out,G-J} = b_{out,G-J} / \cos\left(\frac{\pi(90-\varphi)}{180}\right) \quad (21a,b)$$

For the uncertainty analysis, the path length $L_{in} = L_{in,G-J}$ and $L_{out} = L_{out,G-J}$, actually wall to wall length, are used.

e) Handling of crossed paths of a layer

Assuming no cross flow influence and slow time variation in the layer velocity compared to the ping rate (repetition rate) of the acoustic pulses together with the assumption from Section 6.3d) one gets with equation (3)

$$v_{ax_{path_i}} \cong v_{ax_{path_{i+4}}} = v_{ax_i} \quad \rightarrow \quad v_{ax_i} = \frac{v_{ax_{path_i}} + v_{ax_{path_{i+4}}}}{2} = \frac{v_{ax_i} + v_{ax_i}}{2} = v_{ax_i} \quad i=1, \dots, 4 \quad (22)$$

f) Split error calculation

The error analysis is broken up in 3 parts, following the three basic equations

- Equation (19): Axial path velocity calculation (simplified equation (1))
- Equation (22): axial layer velocity calculation (simplified equation (2))
- Equation (7) simplified with all the above assumptions

This split is a simplification as the same error sources (e.g. lengths, angles) may occur in different equations and are treated individually in block I and II.

g) Chosen error model

The chosen error model is split in two blocks. Figure 8 shows the two blocks with the primary error sources, the intermediate velocity error source and the flow output error. Block II contains the handling of equations (22) and (7).

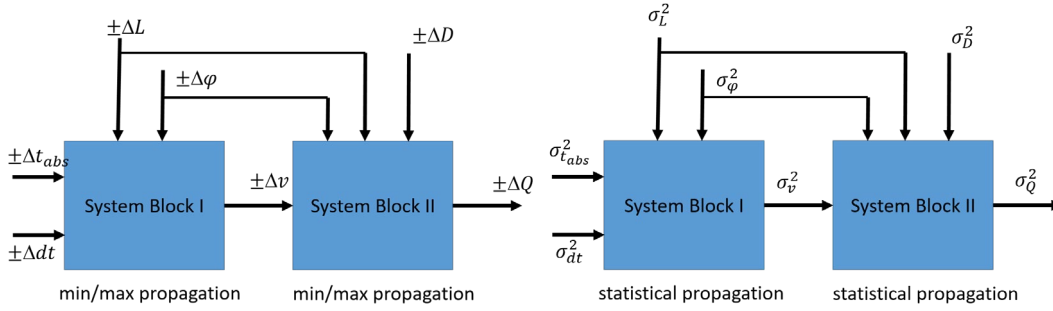


Figure 8a: min/max error propagation model

Figure 8b: statistical error propagation model

7 Error analysis with min/max error bands

The error bands $\pm\Delta, \Delta > 0$ are taken over from section 5. All error contributions are taken positive.

7.1 Single axial path velocity

From equation (19) one gets for a single axial path velocity $v_{ax} = v_{ax_{path}}$

$$v_{ax} = f(L, \varphi, dt, t_{abs}) = \frac{L}{2\cos(\varphi)} \frac{dt}{t_{abs}^2} \quad (23)$$

The error propagation is then given by:

$$\frac{\Delta v_{ax}}{v_{ax}} = \frac{\Delta L}{L} + \tan(\varphi) \frac{\pi}{180} \Delta\varphi + \frac{\Delta dt}{dt} - 2 \frac{\Delta t_{abs}}{t_{abs}} \quad (24)$$

a ₁	a ₂	a ₃	a ₄
$\frac{1}{L}$	$\tan(\varphi) \frac{\pi}{180}$	$\frac{1}{dt}$	$-2 \frac{1}{t_{abs}}$

Table 1: coefficient of the error propagation for the normalized velocity error

In total, there are four different error contributions to the axial layer velocity, consisting of products of the form $a_i \Delta_i$, $i=1, \dots, 4$. For the min/max error analysis all quantities have to be taken positive (absolute values):

$$e_{v_{min/max}} = \frac{\Delta v_{ax}}{v_{ax}} = a_1 \Delta L + a_2 \Delta\varphi + a_3 \Delta dt + |a_4| \Delta t_{abs} \quad (e_{v_{min/max}} = \text{relative error}, \Delta v_{ax} = \text{absolute error})$$

$$e_{v_{min/max}} = \frac{\Delta v_{ax}}{v_{ax}} = e_{v_L_{min/max}} + e_{v_\varphi_{min/max}} + e_{v_{dt}_{min/max}} + e_{v_{t_{abs}_{min/max}}} \quad (25a,b)$$

The inner and outer path lengths are distinguished as well as the inner and outer the axial layer velocities v_{ax} . The two inner and the two outer axial layer velocities are assumed to be identical. For each assumed nominal axial velocity v_{ax} , a Δv_{ax} is calculated for a corresponding uncertainty band:

$$\Delta v_{ax,1} = \Delta v_{ax,4} = \Delta v_{ax,out} \quad \text{and} \quad \Delta v_{ax,2} = \Delta v_{ax,3} = \Delta v_{ax,in} \quad (26a,b)$$

$$\Delta v_{ax,1} = \Delta v_{ax,4} = v_{ax,out} \cdot \Delta v_{ax,out} \quad \Delta v_{ax,2} = \Delta v_{ax,3} = \Delta v_{ax,in} \cdot v_{ax,in} \quad \text{in absolute terms} \quad (26c,d)$$

These bands are then used as input error bands for the error propagation of Q additionally to the ones for D , L and φ .

7.2 Axial layer velocity for crossed paths per layer

With the assumption of section 6.3.e) the error propagation for equation (22) gets with identical maximum error for both paths $\Delta v_{ax,path_i} = \Delta v_{ax,path_{i+4}} = \Delta v_{ax,path}$

$$\frac{\Delta v_{ax,i}}{v_{ax,i}} = \frac{\Delta v_{ax,path_i}}{2 \cdot v_{ax,i}} + \frac{\Delta v_{ax,path_{i+4}}}{2 \cdot v_{ax,i}} = \frac{\Delta v_{ax,path}}{v_{ax,i}} \quad (27)$$

Under the given assumption, the crossed paths therefore behave like a single path in worst case.

7.3 Error propagation for Q

The error propagation for Q with all the above assumptions yields the following expression:

$$Q = \frac{D}{2} \sin(\varphi) \{w_{out} L_{out} (v_{ax,1} + v_{ax,4}) + w_{in} L_{in} (v_{ax,2} + v_{ax,3})\} \quad (28a)$$

$$Q = f(D, \varphi, L_{out}, L_{in}, v_{ax,1}, v_{ax,2}, v_{ax,3}, v_{ax,4}) \quad (28b)$$

By adding up again all the error contributions from the same source of error in a worst case manner (e.g. all $\Delta \varphi_i = \Delta \varphi$) a complicated expression for the relative error propagation of equation (28) is obtained:

$$\begin{aligned} \frac{\Delta Q}{Q} = & \underbrace{\frac{\Delta D}{D}}_{b_1} + \underbrace{\cotan(\varphi) \frac{\pi}{180} \Delta \varphi}_{b_2} + \underbrace{\frac{w_{out} (v_{ax,1} + v_{ax,4})}{w_{out} L_{out} (v_{ax,1} + v_{ax,4}) + w_{in} L_{in} (v_{ax,2} + v_{ax,3})} \Delta L_{out}}_{b_3} \\ & + \underbrace{\frac{w_{in} (v_{ax,2} + v_{ax,3})}{w_{out} L_{out} (v_{ax,1} + v_{ax,4}) + w_{in} L_{in} (v_{ax,2} + v_{ax,3})} \Delta L_{in}}_{b_4} \\ & + \underbrace{\frac{w_{out} L_{out}}{w_{out} L_{out} (v_{ax,1} + v_{ax,4}) + w_{in} L_{in} (v_{ax,2} + v_{ax,3})} 2 \Delta v_{ax,out}}_{b_5} \\ & + \underbrace{\frac{w_{in} L_{in}}{w_{out} L_{out} (v_{ax,1} + v_{ax,4}) + w_{in} L_{in} (v_{ax,2} + v_{ax,3})} 2 \Delta v_{ax,in}}_{b_6} \end{aligned} \quad (29a)$$

b ₁	$\frac{1}{D}$
b ₂	$\cotan(\varphi) \frac{\pi}{180}$
b ₃	$\frac{w_{out} (v_{ax,1} + v_{ax,4})}{w_{out} L_{out} (v_{ax,1} + v_{ax,4}) + w_{in} L_{in} (v_{ax,2} + v_{ax,3})}$
b ₄	$\frac{w_{in} (v_{ax,2} + v_{ax,3})}{w_{out} L_{out} (v_{ax,1} + v_{ax,4}) + w_{in} L_{in} (v_{ax,2} + v_{ax,3})}$

b_5 (2 times for each 2 in dependent layer)	$\frac{w_{out}L_{out}}{w_{out}L_{out}(v_{ax,1} + v_{ax,4}) + w_{in}L_{in}(v_{ax,2} + v_{ax,3})}$
b_6 (2 times for each 2 independent layer)	$\frac{w_{in}L_{in}}{w_{out}L_{out}(v_{ax,1} + v_{ax,4}) + w_{in}L_{in}(v_{ax,2} + v_{ax,3})}$

Table 2: coefficients of the error propagation for the normalized flow error for min/max error analysis

There are total 6 different error contributions to the flow uncertainty, consisting of products of the form $b_i \cdot \Delta_i$ $i=1, \dots, 6$.

$$\frac{\Delta Q}{Q} = b_1 \Delta D + b_2 \Delta \varphi + b_3 \Delta L_{out} + b_4 \Delta L_{in} + 2 * b_5 \Delta v_{ax,out} + 2 * b_6 \Delta v_{ax,in} \quad (29b)$$

$$e_{Q_{min/max}} = e_{Q_D_{min/max}} + e_{Q_\varphi_{min/max}} + e_{Q_{Lout_{min/max}}} + e_{Q_{Lin_{min/max}}} + e_{Q_{vax,out_{min/max}}} + e_{Q_{vax,in_{min/max}}} \quad (29c)$$

(*100 in %)

$$\Delta Q = Q \cdot e_{Q_{min/max}} \quad (29d)$$

8 Statistical error analysis

This approach follows the procedure of GUM [7],[8]), which converts all systematic uncertainties to random variables with a probability density function. Therefore, the probability distribution for all the input error variables is assumed to be uniform. This gives a more conservative bound than the pure Gaussian approximation as was derived in Section 5. Additionally, the result for the standard deviation for velocity and flow becomes conservative due to the following reasons: The statistical uncertainty analysis is done in two steps. First the variance and standard deviation of the assumed Gaussian axial velocity distribution is evaluated by using equation (25) for the velocity. Second the equation (29) for the variance and standard deviation for the flow Q is used. By squaring all the a_i and b_i and multiplying by the corresponding variances of the distributions of the error variables one would get a too pessimistic variance for the results of equations (30) and (31) because by pursuing this approach the errors from the same error sources are assumed to be maximally positively correlated. To compensate for this fact, the error bounds of the uniform distributions of $\Delta v_{ax,out}$ and $\Delta v_{ax,in}$ are chosen as $\frac{\Delta v_{ax,out}}{v_{ax,out}} = \frac{\Delta v_{ax,in}}{v_{ax,in}} = e_{v_\sigma}$ instead of $\sim 2 \cdot e_{v_\sigma}$ which makes these error contributions in equation (30) smaller.

The normalized standard deviation of the axial velocity distribution (evaluated for inner and outer path velocities) is then given by:

$$e_{v_\sigma} = \frac{\sigma_{vax}}{v_{ax}} = \sqrt{(a_1^2 \Delta L^2 + a_2^2 \Delta \varphi^2 + a_3^2 \Delta dt^2 + a_4^2 \Delta t_{abs}^2)/3} \quad (30)$$

where terms $\frac{\Delta L^2}{3}$ etc. correspond to the variances of the uniform distribution.

The normalized standard deviation of the flow distribution is then given by:

$$e_{Q_\sigma} = \frac{\sigma_Q}{Q} = \sqrt{(b_1^2 \Delta D^2 + b_2^2 \Delta \varphi^2 + b_3^2 \Delta L_{out}^2 + b_4^2 \Delta L_{in}^2 + 2 * b_5^2 \Delta v_{ax,out}^2 + 2 * b_6^2 \Delta v_{ax,in}^2)/3}$$

$$e_{\sigma,Q} = \frac{\sigma_Q}{Q} = \sqrt{e_{\sigma,QD}^2 + e_{\sigma,Q\varphi}^2 + e_{\sigma,Q_{Lout}}^2 + e_{\sigma,Q_{Lin}}^2 + e_{\sigma,vax,out}^2 + e_{\sigma,vax,in}^2} \quad (31)$$

The 95% confidence interval for the flow uncertainty is then given by: $\pm 2e_{\sigma,Q}$

The normalized (relative) standard deviation $\frac{\sigma_Q}{Q}$ of Q varies depending on what kind of correlation between the variation of the error from the same sources is assumed and what type of probability density distribution function is used for the axial layer velocity variation. The obtained results are always better than the bounds obtained by the min/max method, and the improvement factor for the 95% confidence interval estimates compared to the min/max error bounds lies roughly in between ~ 1.5 to 4 .

9 NDD example

The presented and proposed method was applied to the installation of an ADM system in the pump-turbine project of Nant de Drance in Wallis, Switzerland. The general project is presented in the contribution [6] of this workshop

9.1 Geometrical and flow data

The acoustic transit time flow meters are located in straight conduit sections as indicated in figures 9 and 10. The exact path lengths of the 8 paths as measured in conduit 1 at Nant de Drance are tabulated in Table 3. As the configuration is 2E8P (crossed paths on 4 layers) with path angles all close to 45°, the ideal situation is such that the four crossed paths configurations are all aligned under the same crossed green lines of Figure 9. The four layers are located at the heights given in Figure 10. For the ideal situation, the four path lengths of the inner paths each would have the same length and the four lengths of the outer paths would each have the same length. As can be seen from Figure 9 and Table 3 the inner (longer, closer to the center) path lengths are almost equal, while the outer (shorter) path lengths differ more because the location of the sensors (R1 to R2 and R7 to R8 for example) are not identical. For the uncertainty analysis these differences however do not play a significant role. Without loss of accuracy in the uncertainty analysis, one can assume an approximate average outer and inner path length (L_{in} und L_{out}) and circular shape without the neglecting the flat bottom.

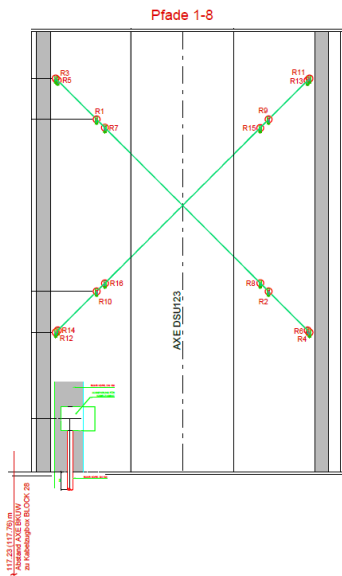


Figure 9: horizontal cut in conduit DSU 456 at Nant de Drance

Path parameters				
	Path angle [°]	Path length L_i [mm]	Protrusion length L_T [mm]	Path length wall to wall $L_i - L_T$ [mm]
Path 1	44.96	7070.4	-123.25	7193.6
Path 2	45.02	10431.7	-89.00	10520.7
Path 3	44.97	10270.9	-103.16	10374.1
Path 4	44.99	6390.8	-134.48	6525.3
Path 5	45.08	7062.7	-121.27	7183.9
Path 6	45.05	10428.0	-89.88	10517.9
Path 7	45	10263.5	-103.42	10366.9
Path 8	45.05	6375.4	-139.15	6514.5

Table 3: path lengths from pill to pill for L_1 to L_8 as measured in conduit DSU 456

The measured path lengths wall to wall $L_{wi,meas}$ are obtained by taking the protrusion effect L_{Ti} into account. For the averaged values, the following values result:

average of measured inner path length pill to pill
average of measured outer path length pill to pill

$$L_{in,meas}: \sim 10.35m$$

$$L_{out,meas}: \sim 6.73m$$

all path angles $\varphi_i: \sim 45^\circ$ [44.96°.....45.08°]
pipe diameter $D: 7.73458m$

$$\varphi_{average} = 45.015^\circ \quad (32)$$

For the uncertainty analysis, the path length $L_{in} = L_{in,G-J}$ and $L_{out} = L_{out,G-J}$, actually wall to wall length are used: $L_{in} = 10.40\text{m}$ $L_{out} = 6.43\text{m}$. The differences to the measured path lengths are irrelevant for the analysis.

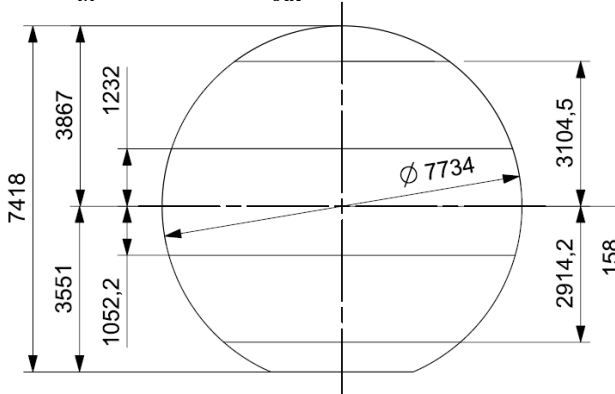


Figure 10: vertical cut conduit DSU 456 at Nant de Drance [6]

The path at the given heights as shown in Figure 10, are assumed to lie in horizontal planes. This is reasonable due to the very small differences ($\sim\text{mm}$) for example R1, R2, R9 and R10.

Given flow rates mean velocity for circular pipe (the straight bottom is not taken into account)

Q_{max} = 60 m³/s (for one turbine)	v_{max} = 1.2766m/s
Q_{min} = 20 m³/s (for one turbine)	v_{min} = 0.4255m/s
Q_{Pump} = 50 m³/s	v_m = 1.064m/s

From the measurement of length and angle measurements, the following error bounds for length, diameter and angle can be assumed as:

- $\Delta L = 2\text{mm} = 0.002\text{m}$ This error bound is also confirmed by independent length determination derived from the absolute transit time measurements
- $\Delta D = 5\text{mm} = 0.005\text{m}$
- $\Delta\phi = 0.06^\circ$ from equation (32)

9.2 Time measurements

a) Absolute transit times t_{abs}

The absolute transit time for a speed of sound c of 1430m/s are for the inner and outer paths in milliseconds [ms]:

$$t_{abs_in} = 0.0073 \text{ sec} = 7.3 \text{ ms} \quad t_{abs_out} = 0.0045 \text{ sec} = 4.5 \text{ ms}$$

Both times are indicated in Figure 11 as dots. An average value of $t_{abs} = 5.9\text{ms}$ can be used for the uncertainty analysis. As both absolute times of $\sim 6\text{ms}$, the specification of the accuracy for the absolute time measurement is much less restrictive (order of 3 decades) compared to the measurement of the transit time differences (see section 2.1).

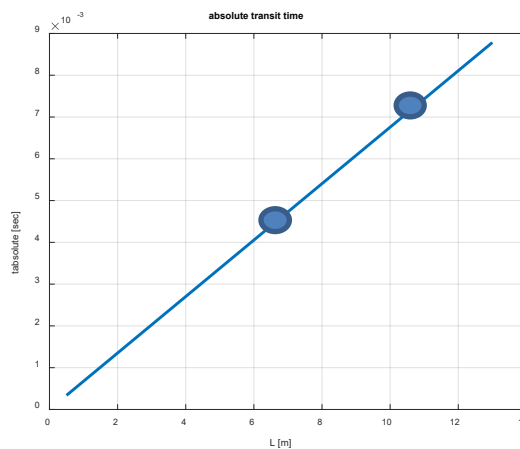


Figure 11: Absolute transit times

The installed measurement system works with the following key characteristics for the data acquisition of the transit times: A transmitter frequency of 1MHz, that means a period of 1 microsecond, a sampling frequency of 10MHz, that means a sampling time of 100 nanoseconds (10 samples per period) and additional sophisticated signal processing. As

the absolute transit times are estimated by subtracting a multiple of half periods from the peak amplitudes of the incoming signals, it can be assumed that the absolute transit times have error bounds of +/- 500 nanoseconds (see Section 2.1 equation (4)):

$$\Delta t_{abs} = 0.5 \mu s.$$

b) Transit time differences dt

The transit time difference is obtained via a correlation method of the forward and return signal. The achieved time resolution is of the order of 1 Nanosecond. For the accuracy of dt the product of flow velocity v and path length L is decisive. With given inner and outer path lengths and min/max velocities, the following transit time differences result:

$$\begin{aligned} dt_{v_{min}L_{in}} &= 3.062e-06 \text{ sec} \\ dt_{v_{max}L_{in}} &= 9.187e-06 \text{ sec} \end{aligned}$$

$$\begin{aligned} dt_{v_{min}L_{out}} &= 1.832e-06 \text{ sec} \\ dt_{v_{max}L_{out}} &= 5.678e-06 \text{ sec} \end{aligned}$$

These time durations are marked in Figure 12, lying on a line. They all lie in a range of 1 to 10 microseconds. The lower two values belong to the minimum velocity, the upper values to the maximum velocity. As the time durations are above 1 Microsecond, the dt measurement is not in a critical range of a few Nanoseconds.

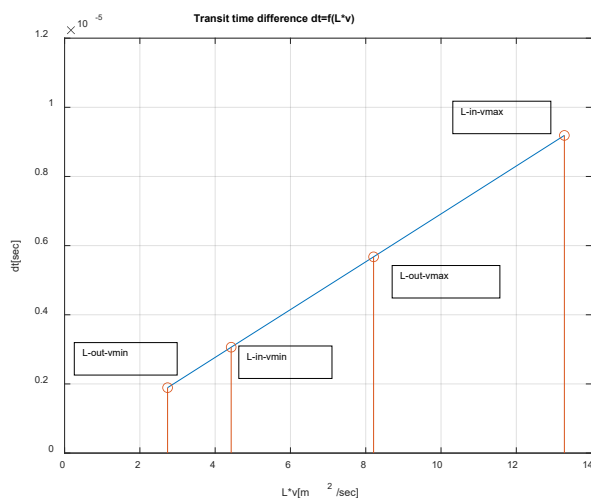


Figure 12: transit time differences dt as a function of $v*L$

The uncertainty analysis is carried out for the inner and outer paths of each velocity separately. The uncertainty of the dt -measurement is in the order of 1 to 2 nanoseconds (see section 2.1, equation (6)). The upper bound is used: $\Delta dt = 2 \text{ ns}$. $v_{min} = 0.4255 \text{ m/s}$ or $v_{max} = 1.2766 \text{ m/s}$ are used for all the layers (uniform velocity profile). For each assumed axial velocity, a Δv_{ax} is calculated for a corresponding uncertainty band:

$$\Delta v_{ax,1} = \Delta v_{ax,4} = \Delta v_{ax,out} \text{ and } \Delta v_{ax,2} = \Delta v_{ax,3} = \Delta v_{ax,in}$$

	$\Delta L = 0.002m$ $\Delta D = 0.005m$ $\Delta \varphi = 0.06^\circ$ $\Delta dt = 2 \text{ ns}$ $\Delta t_{abs} = 0.5 \mu s$ $v = v_{min}$	$\Delta L = 0.002m$ $\Delta D = 0.005m$ $\Delta \varphi = 0.1^\circ$ $\Delta dt = 2 \text{ ns}$ $\Delta t_{abs} = 0.5 \mu s$ $v = v_{max}$	$\Delta L = 0.002m$ $\Delta D = 0.005m$ $\Delta \varphi = 0.06^\circ$ $\Delta dt = 2 \text{ ns}$ $\Delta t_{abs} = 0.5 \mu s$ $v = v_{min}/2$	$\Delta L = 0.002m$ $\Delta D = 0.005m$ $\Delta \varphi = 0.06^\circ$ $\Delta dt = 2 \text{ ns}$ $\Delta t_{abs} = 0.5 \mu s$ $v = v_{min}/5$	$\Delta L = 0.002m$ $\Delta D = 0.005m$ $\Delta \varphi = 0.06^\circ$ $\Delta dt = 2 \text{ ns}$ $\Delta t_{abs} = 0.5 \mu s$ $v = 1.4 v_{max}$
$e_{Q_{min/max}} [\%]$	± 0.413	± 0.362	± 0.484	± 0.718	± 0.354

e_{σ,Q_D}	0.0373	0.0373	0.0373	0.0373	0.0373
$e_{\sigma,Q\phi}$	0.0605	0.0605	0.0605	0.0605	0.0605
$e_{\sigma,QLout}$	0.0050	0.0050	0.0050	0.0050	0.0050
$e_{\sigma,QLin}$	0.0080	0.0080	0.0080	0.0080	0.0080
$e_{\sigma,Qvax,out}$	0.0165	0.0042	0.0516	0.2921	0.0029
$e_{\sigma,Qvax,in}$	0.0357	0.0104	0.0960	0.4872	0.0073
$e_{\sigma,Q}[\%]$	0.0908	0.0734	0.170	0.807	0.073
95% confidence interval	$\pm 0.1816\%$	$\pm 0.1468\%$	$\pm 0.340\%$	$\pm 1.614\%$	$\pm 0.145\%$
99% confidence interval	$\pm 0.2724\%$	$\pm 0.2202\%$	$\pm 0.510\%$	$\pm 2.421\%$	$\pm 0.2175\%$

Table 4: Resulting uncertainties for the flow determination from the transit time and transit time differences measurements, min/max error bands and confidence intervals for different flows: $\frac{v_{min}}{5}$, $\frac{v_{min}}{2}$, v_{min} , v_{max} , $1.4v_{max}$

9.3 Uncertainty results for $e_{\sigma,Q}[\%]$ and $e_{Q,min/max}[\%]$

The important results are highlighted in green in Table 4 for Flow range of interest. The min/max uncertainty is below $\pm 0.42\%$, while the 95% confidence interval is below $\pm 0.19\%$. If the error bounds for velocity were not reduced, the statistical bounds would increase by $\sim 40\%$, while the min/max uncertainty would stay constant. The low uncertainty is mainly due to the facts

- that the product of $L \cdot v$ is in a medium range
- that the geometrical uncertainties are small, especially in the angles.

Figure 13 and 14 show graphically the dependency of the min/max bound for the flow and the standard deviation σ (resp. 2σ) for different flows (velocities). Below $20 \text{ m}^3/\text{s}$ a strong increase can be seen for both quantities. Between 20 and $90 \text{ m}^3/\text{s}$ the decrease is small and levels off. The offset is nondependent of the velocities and only due to geometrical uncertainties.

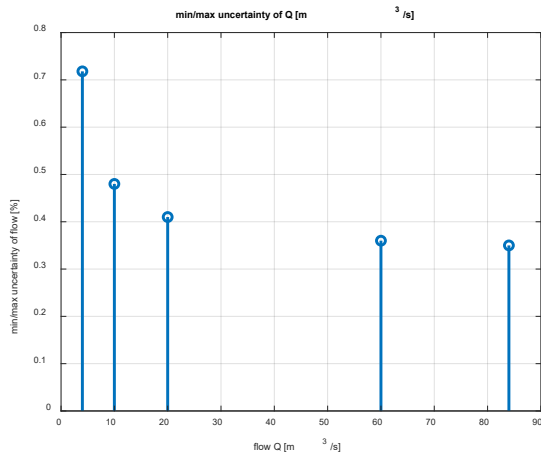


Figure 13: min/max uncertainties (error bounds) for the flow dependent on the velocity (flow)

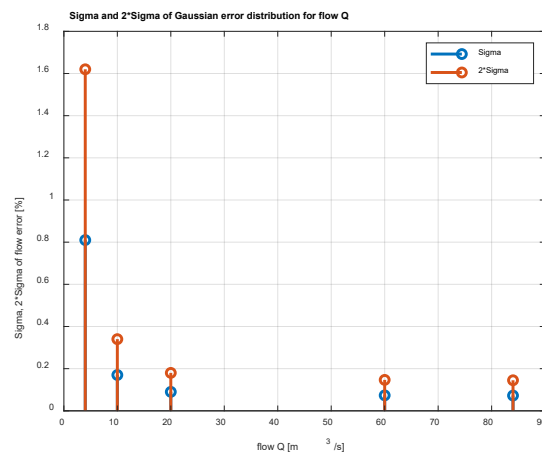


Figure 14: σ and 2σ for the flow error assuming Gaussian distribution dependent on the velocity (flow)

9.4 Overall uncertainty $e_{\sigma,Q,total}$

a) Integration error: e_{int}

$$\sigma_{int} = \frac{\Delta_{int}}{\sqrt{3}} \quad \pm \Delta_{int} \text{ in \% to nominal flow (conservative estimate from [6]: 0.2\%)}$$

b) *Protrusion error: e_{prot}*

The protrusion error can be neglected because the path lengths of greater than 6m allow to neglect the influence of the flow field distortion around the sensors (protrusion length $\sim 0.08m$).

$$\sigma_{prot} = 0$$

c) *Ambient influences: e_{amb}*

The ambient influences are treated as Gaussian distributed random variables with a zero mean and a given standard deviation of

$$\sigma_{amb} \quad \text{in \% to nominal flow (e.g.=0.1)}$$

d) *Unsteady flow conditions: $e_{unsteady}$*

The unsteady flow conditions are combinations of trend, periodic and random contributions. The main remedy of such disturbances is signal processing, especially averaging and trend estimation. Such measures are in place in the measurement unit, as the data acquisition is fast ($>10MHz$) and the flow readings are updated every second. In cases of periodic variations as it seems to be the case in this installation, a longer time interval (\sim several minutes) for averaging the flow measurement readings is recommended. The uncertainty is assumed to be uniformly distributed in a symmetrical uncertainty band:

$$\sigma_{unsteady} = \frac{\Delta_{unsteady}}{\sqrt{3}} \pm \Delta_{unsteady} \text{ in \% to nominal flow (pump 0.1, turbine 0.2, estimate from section 4, report 1)}$$

d) *Overall statistical uncertainty: confidence interval 95% of $e_{\sigma,Q,total}$ [%]*

The overall uncertainty is obtained by applying equation (18) and taking the square root, For the flow uncertainty the value for minimal velocity is used.

$$e_{\sigma,Q,total} = \sqrt{\sigma_{\sigma,Q}^2 + \sigma_{int}^2 + \sigma_{amb}^2 + \sigma_{unsteady}^2}$$

In pump mode:

$$e_{\sigma,Q,total} = \sqrt{0.0908^2 + 0.2^2/3 + 0.1^2 + 0.1^2/3}$$

$$e_{\sigma,Q,total} = 0.1868$$

The 95% confidence interval is: $\pm 0.374\%$

In turbine mode:

$$e_{\sigma,Q,total} = \sqrt{0.0908^2 + 0.2^2/3 + 0.1^2 + 0.2^2/3}$$

$$e_{\sigma,Q,total} = 0.2120$$

The 95% confidence interval is: $\pm 0.424\%$

10 Conclusions

A comprehensive summary of the main error sources that are present if an ADM system for the flow measurement is used. The equations for evaluating Q from transit time measurements are given. The complex calculation for Q with 49 error variables is then simplified by in most cases reasonable assumptions. The error propagation is performed along these simplified equations by splitting the error contribution in separate blocks. The min/max error propagation is carried out by assigning for each input error symmetrical bounds which correspond to the given uncertainty bounds. By using always maximum conditions in the dependency of the individual error variations for the same type of error variables an upper bound for the uncertainty of the flow calculation can be found.

For the statistical approach several questionable assumptions on correlation between the error variations for the same type of error variables must be made. Depending on the degree of correlation (correlation coefficient r assumed to be between 0 and 1) the 95% confidence interval varies considerably. The intervals are for the flow range of $20m^3/s$ to $80m^3/s$ however always smaller (improvement by factor 1.5 for fully correlated to 4 for fully uncorrelated) than the one obtained by the min/max method. As the fully uncorrelated assumption is too optimistic and the fully correlated too pessimistic for the statistical approach, an assumption is appropriate that leads to a result in the middle. This leads then to an improvement factor of ~ 2.5 for the 95% confidence interval compared to the min/max approach. The analysis shows that by treating deterministic variables as random, several statistical decisions about independency and mutually uncorrelated variables

have to be made. For small flows (less than $10\text{m}^3/\text{s}$) the statistical uncertainty obtained with the applied approach seems to surpass the min/max error bound.

The presented material shows that for a serious application of the error propagation for deterministic systematic errors in the determination of Q , the following points have to be considered:

- Obtain as much knowledge of the deterministic errors as possible
- Question the simplification and the assumption in the equations
- Question the splitting methodology for sequential propagation of the error
- Analyse the error bounds for the min/max method
- Analyse the statistical uncertainties for minimal ($r=0$) and maximal ($r=1$) correlation of the corresponding variables. Is a $r<0$ possible?
- Find a reasonable compromise between the correlation of the input error variables
- Use of uniform probability density functions for input error variables of systematic unknown but bounded origin.

For the overall uncertainty, a flow measurement is also exposed to random variations in time of ambient conditions which are described by Gaussian independent random variables whereas the integration error evaluated by CFD analysis can be described by uniform or Gaussian density functions depending on the knowledge of the individual case.

Acknowledgement

The author would like to thank the Rittmeyer company for providing the data as a basis for the error analysis, as well as the pumped storage plant Nant de Drance SA for permission to present the results in this paper.

References

- [1] Standard IEC 60041:1991
- [2] Tresch, Th. Gruber P., Staubli T.: "Uncertainty analysis of the acoustic method with respect to absolute travel time and time difference determination", IGHEM 2004, Lucerne, Switzerland
- [3] Th. Tresch, P. Gruber, Th. Staubli: "Comparison of integration methods for multipath acoustic discharge measurements", IGHEM 2006, Portland, USA
- [4] Tresch Th., Lüscher B., Staubli T., Gruber P.: "Presentation of optimized integration methods and weighting corrections for the acoustic discharge measurement", IGHEM 2008, Milano, Italy
- [5] Hoffmann J.: *Taschenbuch der Messtechnik*, Fachbuchverlag Leipzig, Hanser Verlag, 4. Auflage 2004
- [6] Staubli T., Fahrni F.: "Analysis of the Flow Conditions in the Nant de Drance Pumped Storage Plant and their Impact on Acoustic Discharge Measurement", IGHEM 22, Grenoble, France
- [7] GUM Guide to the Expression of Uncertainty in Measurement, chapter 4, https://www.iso.org/sites/JCGM/GUM/JCGM100/C045315e-html/C045315e_FILES/MAIN_C045315e/04_e.html
- [8] GUM Guide to the Expression of Uncertainty in Measurement chapter 5, https://www.iso.org/sites/JCGM/GUM/JCGM100/C045315ehtml/C045315e_FILES/MAIN_C045315e/05_e.html
- [9] Andersson U., Dahlbäck N., Sundqvist P.: "Accuracy of an absolute method used for relative measurements: Study of an acoustic transit time method", IGHEM 2010, Roorkee, India